Spatially explicit assessment of water stress and potential mitigating solutions in a large water-limited basin: the Yellow River basin in China

Weibin Zhang[1,2], Xining Zhao[3,4], Xuerui Gao[4], Wei Liang[5], Junyi Li[5], and Baoqing Zhang[6*]

[1]College of Water Resources and Architectural Engineering, Northwest A&F University, 712100 Yangling, Shaanxi Province, China.

[2]Key Laboratory of Agricultural Soil and Water Engineering in Arid and Semiarid Areas, Ministry of Education, Northwest A&F University, 712100 Yangling, Shaanxi Province, China.

[3]Institute of Soil and Water Conservation, Northwest A&F University, 712100 Yangling, Shaanxi Province, China.

[4]Institute of Soil and Water Conservation, Chinese Academy of Sciences and Ministry of Water Resources, 712100 Yangling, Shaanxi Province, China.

[5]School of Geography and Tourism, Shaanxi Normal University, 710119 Xi'an, Shaanxi Province, China.

[6]Key Laboratory of Western China's Environmental Systems (Ministry of Education), College of Earth and Environmental Sciences, Lanzhou University, 730000 Lanzhou, Gansu Province, China.

***Corresponding author:**

Email: baoqzhang@lzu.edu.cn;

Tel (Fax): +86 (931) 8912404;

Address: NO. 222 Tianshui Road (South), Chengguan District, Lanzhou, Gansu Province, China

Abstract:

Comprehensive assessment of the long-term evolution of water stress and its driving factors is essential for designing effective water resource management strategies. However, the role of water withdrawal and water availability components in determining water stress and potential mitigating measures in large water-scarce basins are poorly understood. Here, an integrated analytical framework was applied to the Yellow River basin (YRB), where the water crisis has been a core issue for sustainable development. The analysis suggests that the YRB has experienced unfavorable changes in critical water stress indicators over the past fifty-six years. Compared to the period from 1965 to 1980, the regional water stress index (WSI), the frequency and duration of water scarcity, increased by 76%, 100%, and 92%, respectively, over the recent two decades. Water withdrawal was the primary driver of the increased WSI before 2000; however, it has since contributed equally with water availability. Meanwhile, local water management and climate change adaptation were shown to be important in determining total water availability at the sub-basin scale. Water demand in the 2030s is predicted to be 6.5% higher than during 2001–2020 (34.2 km^3), based on the trajectory of historical irrigation water use and corrected socio-economic data under different Shared Socioeconomic Pathways (SSPs). To meet all sectoral water needs, a surface water deficit of 8.36 km^3 is projected. Potential improvements in irrigation efficiency could address 25% of this deficit, thereby alleviating the pressure on external water transfer projects. Such efficiency gains would enable the WSI of the YRB in the 2030s to be maintained at the current level (0.95), which would worsen conditions for 44.9% of the total population while easing them for 10.7%, compared to the 2000s. Our results have vital implications for water resource management in basins facing similar water crises to that in the YRB.

1 Introduction

Water resources underpin human life, socio-economic development, and ecosystem health (Oki and Kanae, 2006; Han et al., 2023), but often have an uneven spatiotemporal distribution as well as a mismatch with water demands (Veldkamp et al., 2017; Wang et al., 2020; Scanlon et al., 2023). This problem has been worsened by an increased human water demand during the last few decades, driven by population growth, improving living standards, and expansion of irrigated agriculture (McDonald et al., 2011; Wada et al., 2016b; Huang et al., 2018). Climate change poses an additional threat to already stressed water resources by adding uncertainty, especially in terms of changes in interannual and seasonal precipitation and temperature (Schewe et al., 2014; Rodell and Li, 2023). Water scarcity is challenging the stability and sustainable development of human society in many regions of the world, especially in developing countries (Munia et al., 2020; Huang et al., 2021). Approximately one-third to half of the global population is currently experiencing water scarcity, with most water scarcity occurring in India and China (Mekonnen and Hoekstra, 2016; Qin, 2021). By 2030, half of the global population is predicted to experience severe water stress (UNEP, 2015). Droughts and floods would further intensify water stress, with high-income areas not immune to these threats (Rodell and Li, 2023). Water scarcity results in many social and environmental issues, such as food production reduction, drinking water shortage, and ecosystem health degradation (Porkka et al., 2016; Wang et al., 2017; Long et al., 2020). Thus, it is essential to understand the evolution of water stress and the associated driving factors; this is a prerequisite for designing effective water resource management strategies and achieving Sustainable Development Goal (SDG) target 6.

The Yellow River basin (YRB), the second-largest river basin in China, is known as the "Chinese cradle". It is responsible for 13% of national grain production but only possesses approximately 2% of national water resources (Zhuo et al., 2016). Meanwhile, the reserves of coal and oil in this basin account for 70% and 50% of China's total, respectively (Ma et al., 2020b). The large-scale exploration of energy sources also comes at the cost of a large amount of water usage. Accompanying a boom in

agriculture and prosperous economy, the total water consumption (both surface and groundwater) in the YRB increased by 120% between the 1960s and 2009 (Zhuo et al., 2016). In contrast, natural runoff significantly decreased during the period 1960–1990s, before slightly recovering in recent years (Tang et al., 2013). Owing to climate change-induced natural water availability and intensive human water usage, the YRB has been facing severe water stress (Xie et al., 2020; Niu et al., 2022; Zhang et al., 2023c). This problem has constrained the ecological protection and high-quality development of the YRB, which was stressed as a major national strategy in 2019 by the Chinese government.

Water stress in the YRB has been widely reported in global assessments, which have provided general overviews of water stress for both historical and future periods (Veldkamp et al., 2017; Greve et al., 2018; Qin et al., 2019). However, these estimates were based on data having a coarse spatial resolution, such as a whole river basin or at 0.5° × 0.5° level (Huang et al., 2021). The insights obtained at such spatial resolution might be difficult for water resource managers and policymakers to utilize (Degefu et al., 2018). Moreover, due to the lack of validation of most global hydrological models used to simulate runoff, there may be large biases in water supply assessment. A wealth of previous studies in China have explored the general feature of water stress in the YRB at different spatial scales, ranging from provincial or prefectural (Zhao et al., 2015; Huang et al., 2023), to river basin scale (Yin et al., 2020), to sub-basin scale (Zhou et al., 2019; Xu et al., 2022), to grid scales (Zhuo et al., 2016). Recently, considering quality requirements, a comprehensive series of assessments of nationwide water stress at multiple temporal and geographic scales has been performed in China (Ma et al., 2020a), which has markedly advanced our understanding of current water stress conditions. However, upstream inflows and water consumption were typically not considered in most of these assessments. Neglecting upstream water availability leads to an overestimation of downstream water stress (Munia et al., 2020; Sun et al., 2021). Previous work in China showed that the difference in population affected by severe water stress was 60% with and without consideration of upstream water resources,

which is even larger in northern water-limited areas (Liu et al., 2019). Incorporating upstream flows and water consumption provides a more accurate assessment of water stress in the real world. Some studies have significantly advanced the understanding of water stress in the YRB by accounting for upstream components, reservoir operations, and water transfer projects (Omer et al., 2020; Xie et al., 2020; Albers et al., 2021; Sun et al., 2021). Yet, these studies often covered only short periods (less than 20 years), thereby limiting the comprehensive documentation of the temporal dynamics of water stress. More importantly, human water usage estimates in both the historical and future have mostly been based on macroscale socio-economic data, such as gross domestic product and population (Wada et al., 2016a; Yin et al., 2017; Liu et al., 2019). However, changes in water use efficiency, particularly in irrigation, were not considered. This omission may underestimate the effects of technological factors and water conservancy measures, introducing uncertainties into water stress assessments (Zhou et al., 2020; Huang et al., 2021). A long-term water withdrawal dataset at the prefectural scale, based on nationally coordinated surveys, was recently constructed by Zhou et al. (2020). Utilizing this newly developed dataset could bring new insights into the changing pattern of historical water stress and lead to more reliable future projections. A previous study has explored the spatiotemporal features of water stress in the YRB at finer resolution using this dataset (Zhang et al., 2024). Nevertheless, the role of water withdrawal (i.e., different sectors) and water availability components in determining water stress remains unclear. Meanwhile, potentially feasible solutions in terms of water use efficiency improvement for mitigating future water stress have not been quantified.

Here, we provide a spatially explicit assessment of water stress in the YRB at the sub-basin scale, taking into account environmental flow requirements (EFR) and upstream flows. The objectives of our study were to: (1) assess the evolution of water stress over the past fifty-six years in terms of critical indicators, including the intensity, frequency, duration, and exposed population of water scarcity; (2) identify the dominant driver of changes in water stress during 1965–2020; and (3) quantify future water stress and explore potential solutions. Our findings provide valuable information for

designing policies towards integrated water resource management in the YRB.

2 Materials and methods

Multiple datasets and methods were used to develop an integrated analytical framework, including multi-dimensional water stress indicators (i.e., intensity, duration, frequency, and exposed population), driving factors of changes in historical water stress, and surface water deficits in the future along with potential solutions to address these (Fig. 1). A more detailed description can be seen in the following section.

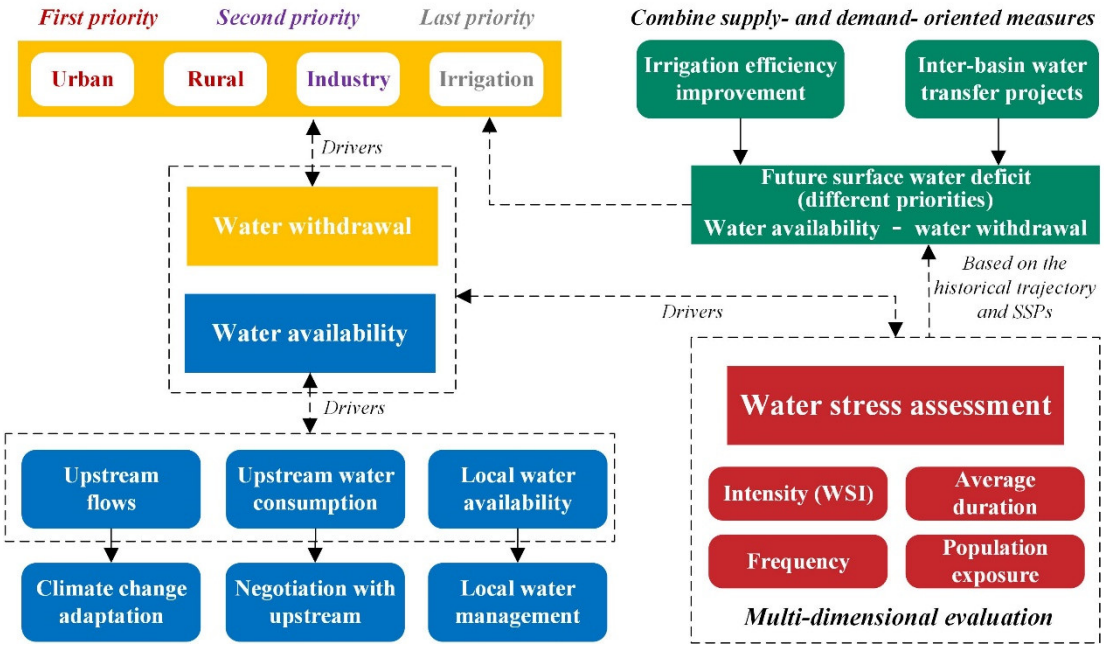

Figure 1. Framework for water stress assessment. The red, orange, blue, and green colors indicate water stress assessment, water withdrawal, water availability, and future surface water deficit, respectively. The rectangles and rounded rectangles indicate the main and detailed components of the aforementioned four parts, respectively. The dashed and solid arrows indicate impact factors and mitigation measures, respectively.

2.1. Study area

The YRB is the second-largest basin in China, with a total drainage area of 79.5×10^4 km^2 and a mainstream length of 5464 km. It runs through nine provinces or

municipalities and three geomorphological units: the Qinghai–Tibet Plateau, Loess Plateau, and North China Plain (Fig. 2). Our study focused on the areas above the Huayuankou hydrological station, the outlet of the middle reaches of the YRB, owing to the negligible runoff downstream of this. Based on the Soil and Water Assessment Tool (SWAT), the study area was further divided into 425 sub-basins (Fig. S1). Most parts of the YRB are arid or semi-arid regions, with the mean annual precipitation being 450 mm. The rapid expansion of irrigated agriculture has induced a very large irrigation water demand, while population growth and socio-economic development have led to an increase in domestic and industrial water use (Zhou et al., 2020), leading to an intensified water crisis in this water-limited basin (Song et al., 2023).

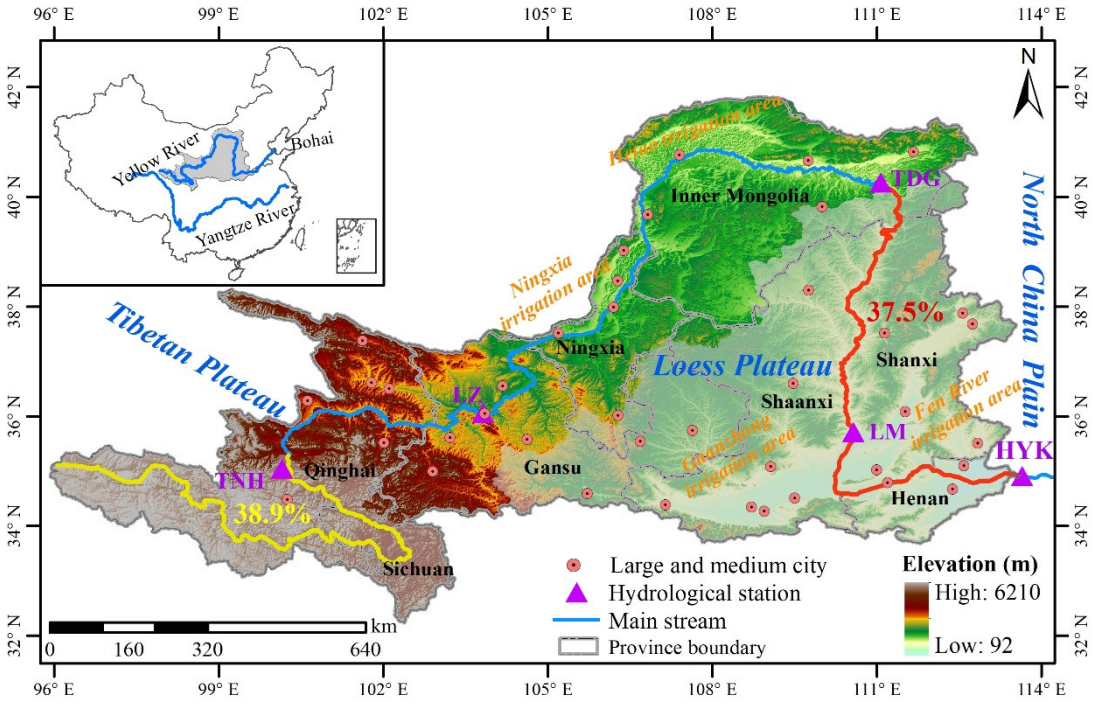

Figure 2. Location of the study area. TNH = Tangnaihai, LZ = Lanzhou, TDG = Toudaoguai, LM = Longmen, and HYK = Huayuankou. Yellow and red numbers indicate the ratio of mean annual natural runoff above the TNH station and the section between TDG and HYK station to that of the HYK station, respectively.

2.2. Critical indicators of water stress

The water stress index (WSI), widely used to assess the water stress intensity, is defined

as the ratio of water withdrawal to water availability (Equation 1). A high WSI value in an area represents high water stress intensity, but not necessarily water scarcity. When the WSI is greater than 1 (WSI>1), water resources cannot sustain environmental or anthropogenic needs and a region is considered to experience water scarcity (Veldkamp et al., 2017; He et al., 2021).

$$\mathrm{WSI}_{i,m} = \frac{WW_{i,m}}{\mathrm{WA}_{i,m}} , \quad (1)$$

where, $WW_{i,m}$ is the total water withdrawal (irrigation, industry, urban, and rural) in sub-basin *i* and month *m*; $\mathrm{WA}_{i,m}$ is the total water availability for sub-basin *i* in month *m*, which consists of the locally generated runoff and incoming discharge from upstream sub-basins taking into account the EFR and upstream water consumption (Liu et al., 2019):

$$\mathrm{WA}_{i,m} = R_{i,m} + \sum_{j=0}^{i}(Q_{j,m} - WC_m) - EFR_{i,m} , \quad (2)$$

where, $R_{i,m}$ is the local water yield, including surface, baseflow, and lateral flow, simulated by the SWAT model; $Q_{j,m}$ is the discharge entering sub-basin *i* from all upstream sub-basins *j* in month *m*; WC_m is the total upstream water consumption in month *m*; and $EFR_{i,m}$ is the environmental flow requirements in sub-basin *i* and month *m*. Pastor et al. (2014) compared and tested different calculation methods for estimating EFR. They demonstrated that the Variable Monthly Flow (VMF) method was most compatible with actual environmental water requirements, distinguishing between low-flow (60% of a water resource allocated to EFR), mediate-flow (45%), and high-flow conditions (30%). Given its performance in the seasonal assessment of water availability (Veldkamp et al., 2017), we therefore adopted the VMF method in our study.

Water stress is more inclusive and broader concept. Based on previous study (Veldkamp et al., 2017), beyond assessing the severity of water stress through the WSI, the frequency and average duration of water scarcity were also used to characterize historical water stress conditions (see Equations 3 and 4):

$$Frequency_i = \frac{NMWS_i}{TM} \ , \tag{3}$$

$$\text{Average } duration_i = \frac{NMWS_i}{NEWS_i} \ . \tag{4}$$

where, $NMWS_i$ is the number of months with WSI>1 in sub-basin *i*; TM is the total number of months in different periods (e.g., 20 years = 240 months); $NEWS_i$ is the number of water scarcity events in sub-basin *i*.

In terms of the population exposed to water scarcity at the sub-basin scale, we categorized sub-basins into four groups with varying WSI values between two consecutive periods: moving into/out of water scarcity and alleviation/aggravation of water scarcity (Table 1).

Table 1. Definitions of different types of population exposed to water scarcity between two periods (WSI_f and WSI_l are WSI values in the former and latter periods, respectively).

WSI value	Classification
WSI_f <1 and WSI_l ≥1	Moving into water scarcity
WSI_f ≥1 and WSI_l <1	Moving out of water scarcity
WSI_f ≥1, WSI_l ≥1, and $WSI_l > WSI_f$	Aggravation of water scarcity
WSI_f ≥1, WSI_l ≥1, and $WSI_l < WSI_f$	Alleviation of water scarcity

2.3. Attribution analysis

To identify the dominant factor affecting the changing pattern of water stress at the sub-basin scale, we first calculated the differences in WSI between consecutive time steps (ΔWSI) at the decadal scale (P1: 1965–1980, P2: 1981–2000, and P3: 2001–2020).

$$\Delta\text{WSI} = \text{WSI}_{t+1} - \text{WSI}_t \ , \tag{5}$$

Then, the relative contributions of water withdrawal (different water use sectors) and water availability (climate change) to changes in WSI (ΔWSI) were obtained by keeping one factor constant, as follows:

$$\Delta \mathrm{WSI}_{WW} = \left(\frac{WW_{t+1}}{WA_t} - \frac{WW_t}{WA_t}\right) / |\Delta \mathrm{WSI}| \ , \quad (6)$$

$$\Delta \mathrm{WSI}_{WA} = \left(\frac{WW_t}{WA_{t+1}} - \frac{WW_t}{WA_t}\right) / |\Delta \mathrm{WSI}| \ , \quad (7)$$

$$Driver_{WSI} = \text{maximum}\ (|\Delta \mathrm{WSI}_{WW}, \Delta \mathrm{WSI}_{WA}|) \ . \quad (8)$$

where, $\Delta \mathrm{WSI}_{WW}$ and $\Delta \mathrm{WSI}_{WA}$ are the contributions of water withdrawal and water availability, respectively.

According to Equation 2, water availability comprises local water availability (ΔLocal WA), upstream flows (ΔUp WA), and upstream water consumption (ΔUp WC). We further explored the relative changes in components of water availability for each sub-basin between two consecutive periods (Munia et al., 2020).

$$\Delta \text{Local WA} = \text{Local WA}_{t+1} - \text{Local WA}_t \ , \quad (9)$$

$$\Delta \text{Up WA} = \text{Up WA}_{t+1} - \text{Up WA}_t \ , \quad (10)$$

$$\Delta \text{Up WC} = \text{Up WC}_{t+1} - \text{Up WC}_t \ , \quad (11)$$

Similarly, the dominant driver of water availability ($Driver_{WA}$) was calculated as follows:

$$Driver_{WA} = \text{maximum}\ (|\Delta \text{Local WA}, \Delta \text{Up WA}, \Delta \text{Up WC}|) \ . \quad (12)$$

Additionally, to assess the impact of vegetation restoration on water availability, we ran the SWAT model with two simulation scenarios. Under a normal scenario, the model was driven by land cover data from 2015 and climatic data from 2001 to 2020. Another scenario was driven by land cover data from 1990, while maintaining the same climatic conditions as in the normal scenario (2001–2020). The WSI and population exposed to water scarcity in P3 have been recalculated.

2.4. Water availability and water use data processing

Natural water availability data for the period 1965–2020 at the sub-basin scale are based

on the SWAT model simulation that have been validated against natural discharges from hydrological stations. Generally, the SWAT model performed well in most cases, with the Nash–Sutcliffe efficiency (NSE) and the coefficient of determination (R^2) exceeding 0.7 for stations along the main stream, and exceeding 0.6 for most stations along the tributaries during the validation period (Fig. S2). Historical annual prefectural-level human sectoral water withdrawal data during 1965–2013, including irrigation, industry, urban, and rural water uses, were obtained from Zhou et al. (2020), which is based on the National Water Resources Assessment Programs (1965–2000) and Water Resources Bulletins (2001–2013). We extended this dataset at the prefectural-level to 2020 by collecting Water Resources Bulletins from various provinces within the YRB. For cities that did not distinguish between urban and rural water use (presented as an aggregate under domestic water use), we disaggregated the data using the 2013 ratio. This annual water withdrawal dataset from 1965–2020 was first disaggregated at the 1-km spatial resolution grid scale according to land use and population density data (https://www.resdc.cn/).

Specifically, irrigation water withdrawal was downscaled based on the irrigated cropland land use and net irrigation requirement, as follows:

$$IRW_{j,m} = \frac{I_{j,m} \times A_j}{\sum_{m=1}^{12} \sum_{k=1}^{N} I_{k,m} \times A_k} \times IRW_a \quad (13)$$

where, $IRW_{j,m}$ is the irrigation water withdrawal of grid cell j in month m; $I_{j,m}$ is the net irrigation requirement of grid cell j in month m for different crops, which was calculated as the difference between the reference crop evapotranspiration and effective precipitation; A_j is the irrigated area; IRW_a is the annual irrigation water withdrawal in the city where grid cell j is located; N is the number of irrigated cropland grid cells in that city.

Similarly, industrial water withdrawal was downscaled according to the maps of industrial and mining land, and assumed equally distributed within a year. The urban and rural water withdrawals were disaggregated based on the urban and rural residential

areas, population density, and a monthly factor:

$$URW_{j,m} = \frac{Pop_j}{\sum_{m=1}^{12}\sum_{k=1}^{N} M_{k,m} \times Pop_k} \times URW_a \times M_{j,m} \quad (14)$$

where, $URW_{j,m}$ is the monthly urban and rural water withdrawals in grid cell j; Pop_j is the population in grid cell j and URW_a is the annual urban and rural water withdrawals in the city where grid cell j is located; $M_{j,m}$ is a monthly factor considering seasonal water use variations (Huang et al., 2018).

Then, the grid-level water withdrawal datasets were aggregated at the sub-basin scale. The detailed calculation process for historical water availability and water withdrawal is described in Zhang et al. (2024).

The annual irrigation water withdrawal at the sub-basin scale for the 2030s (mean value from 2031 to 2040) was estimated based on historical trajectories. Specifically, linear regression was employed to identify the trend in irrigation water withdrawal from 2001 to 2020 (P3 period). If the trend was significant (p<0.05), future irrigation withdrawal was predicted using Equation 15; otherwise, the irrigation water withdrawal for the base year (mean value from 2016 to 2020) was used as the future value.

$$\mathrm{FIR} = \mathrm{IRW_{to}} + trend \times (t - t_0) \quad (15)$$

where, FIR is the future irrigation water withdrawal for each year during 2031–2040; $\mathrm{IRW_{to}}$ is the irrigation water withdrawal for the base year; $trend$ is the linear slope of the irrigation during P3 period.

The projected second industrial value added and population (urban and rural) at the grid scale under the five Shared Socioeconomic Pathways (SSP1–5) during 2020–2040 were used to estimate industrial and domestic water use in the 2030s (Tong et al., 2024). Statistical data at the prefectural level in 2020 from the Statistical Yearbook of various provinces were used as the benchmark to correct the projected industrial value added (IVA) and population under different SSPs. Future industrial water withdrawal was estimated by multiplying the IVA by the water use intensity (Florke et al., 2013; Wada et al., 2016b). The IVA was estimated by multiplying its share of the second industrial

300 value added, and the water use intensity was calculated as follows:

$$\mathrm{WUI}_{ind} = \mathrm{WUI}_{ind,t0} \times (1 - C_{ind})^{t-t0} \quad (16)$$

where, WUI_{ind} is the water use intensity for industry; $\mathrm{WUI}_{ind,t0}$ is the industrial water use intensity for the base year (2020 in this study); C_{ind} is the annual change rate in water use intensity (%), which varies according to different SSPs: 1.1% for SSP1
305 and SSP5, 0.6% for SSP2, and 0.3% for SSP3 and SSP4 (Wada et al., 2016b).

Similarly, urban and rural domestic water withdrawal was estimated by multiplying the population by the domestic water use intensity. The latter was calculated as follows:

$$\mathrm{WUI}_{dom} = \mathrm{WUI}_{dom,t0} + C_{dom} \times (t - \mathrm{t0}) \quad (17)$$

where, WUI_{dom} is urban and rural domestic water use intensity; $\mathrm{WUI}_{dom,t0}$ is the
310 domestic water use intensity for the base year (2020); C_{dom} is the annual change in water use intensity (liter per day per person), which varies according to different SSPs (Hanasaki et al., 2013) (see Table S1).

The future livestock water withdrawal was assumed to be equal to the average of the past five years (2016–2020) due to the general unavailability of related data.

315

2.5. Future water stress and potential solutions

Given the high uncertainty in climate change projections (Greve et al., 2018), we only focused here on the impact of changes in human water usage on water stress. Thus, future water availability in the 2030s was maintained at the same level as the historical
320 P3 period. Because the absolute values of water storage in groundwater aquifers are difficult to estimate and often unknown (Veldkamp et al., 2017; Huang et al., 2021), we calculated only the future surface water deficit by subtracting surface water demand from water availability for each sub-basin. Surface water use was estimated based on its proportion of the total water withdrawal in 2020, which was obtained from the Water
325 Resources Bulletins of each province and the Yellow River. We considered water use

in different sectors. The first priority was urban and rural water demand, the second priority was industrial water demand, and the last priority water was irrigation. From first priority to last priority, greater water stress equated to greater socio-economic loss. Competition between the agricultural and other sectors for water is increasing. Irrigation water usage accounts for the largest proportion of total water demand, which also provides the most practical solution for alleviating water stress across all sectors. Therefore, we collected data on irrigation efficiencies for 2020 and 2025 (target values) at the prefectural scale from the 14th Five-Year Plan for water resources for various cities and provinces within the YRB. Based on previous similar water resource planning documents released by the Chinese government, these irrigation efficiency targets are generally attainable. It thus was assumed that irrigation efficiency would continue to increase at the same rate after 2025, allowing us to project irrigation efficiency into the 2030s (see the relative change in Fig. S3). Next, we estimated future net irrigation water withdrawal (NIR) by multiplying the current irrigation efficiency (2020) by the projected irrigation water withdrawal (Equation 15). The future irrigation water withdrawal, accounting for improved irrigation efficiency, was then calculated by dividing the NIR by the improved irrigation efficiency values. We further quantified the contributions of improved irrigation efficiency to the surface water deficit and water stress in the future.

3 Results

3.1. Multi-dimensional assessment of water stress and attribution of changes in WSI

As shown in Fig. 3a, annual WSI exhibited a rapid upward trend before 2002, followed by a gradual decrease, with water scarcity first occurring in the 1990s (WSI >1). On a decadal scale, the regional WSI increased from 0.55 in P1 to 0.78 in P2 and 0.96 in P3, representing a relative increase of 76% over the entire study period. This exacerbation of water stress was primarily driven by increased water withdrawals from P1 to P2.

However, the contributions of water withdrawals and water availability to the changes in WSI were nearly equal from P2 to P3 (10.4% versus 11%). Water stress hotspots were mainly found in the Lanzhou–Toudaoguai section, characterized by high water demand but limited water availability (Fig. S4). In contrast, water stress was low in regions above Lanzhou station and the middle parts of the Loess Plateau, with annual WSI values < 0.2. The regional average duration and the frequency of water scarcity have almost doubled, increasing from 3 months and 0.25 in P1 to 5.8 months and 0.5 in P3, respectively (Fig. 3b). These indicators showed a similar spatial distribution pattern to that of severity (WSI value). For example, in areas where large irrigated districts or cities are located (e.g., Lanzhou–Toudaoguai section and eastern parts of Shanxi province), the frequency was > 0.6 and average duration was at least four months, with some sub-basins facing year-round water scarcity (Fig. S5).

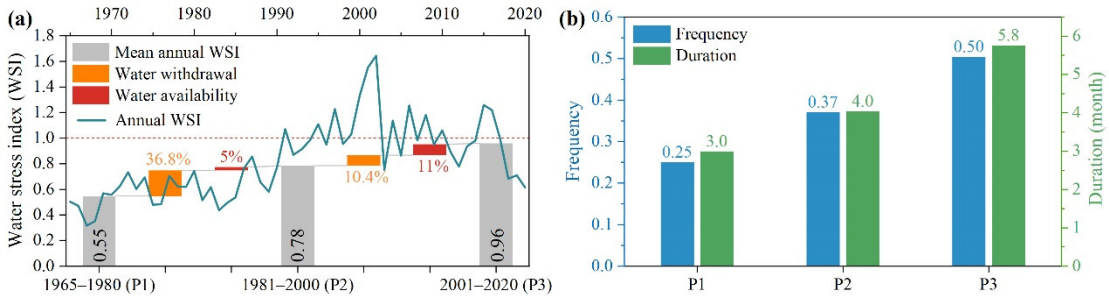

Figure 3. (a) Evolution of the regional water stress index (WSI) and its drivers. (b) Frequency and average duration of water scarcity.

Generally, the change directions of WSI, frequency, and duration presented similar patterns (Figs. 4 and S5c–f). Specifically, most sub-basins experienced increases in WSI from P1 to P2, with the highest increases occurring in the Lanzhou–Toudaoguai section and the Fen River irrigation area (Fig. 4a). From P2 to P3, the areas with the largest increases in WSI were primarily concentrated in the northern part of the YRB and in some cities (Fig. 4b). In contrast, decreases in WSI were observed mainly around the Ningxia irrigation area. Compared to WSI, fewer areas showed decreases in both the frequency and duration of water scarcity (Figs. 4c and 4d). Most sub-basins downstream

of the Lanzhou station experienced increases in both the frequency and duration, with these increases becoming more spatially confined over the past two decades. Further analysis showed that the population moving out of and experiencing alleviation in water scarcity accounted for 0%–7.8% and 3.5%–6.6%, respectively, of the total population during different periods; this was always much lower than the proportion of the population moving into (7.5%–10.3%) or experiencing an aggravation (27.3%–34.7%) in water scarcity in the corresponding periods (Figs. 4e and 4f). Much greater differences were found in the proportion of the population experiencing both changes in frequency and duration of water scarcity; 54.2%–71.2% of the population experienced an increase in both indicators, while only 1% experienced a decrease in both indicators. In summary, changes in critical indicators of water stress suggest that the YRB has been facing an increasingly unfavorable water crisis during the last five decades.

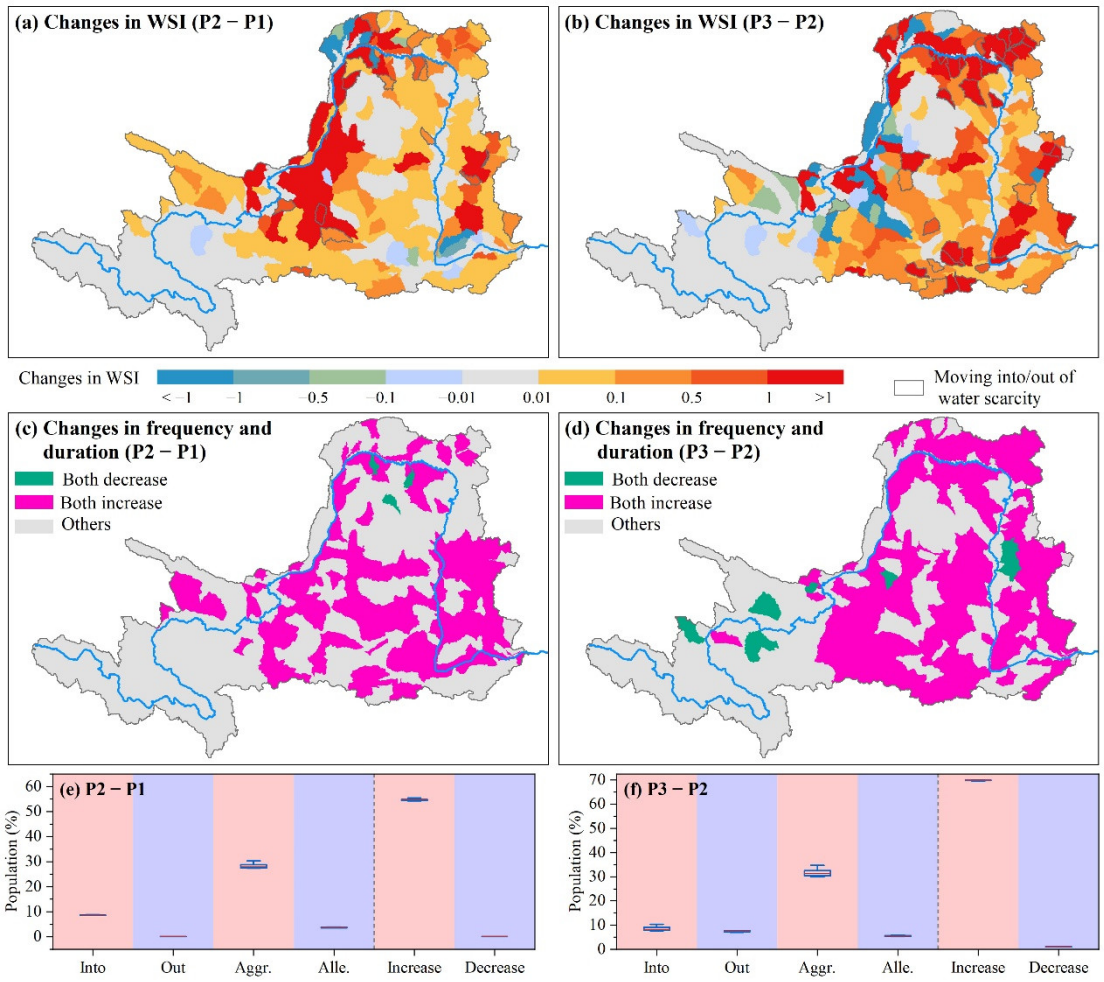

Figure 4. Changes in the (a and b) water stress index (WSI), (c and d) frequency, and duration of water scarcity. (e and f) Proportion of the population moving into (Into)/out of (Out) water scarcity, experiencing aggravated (Aggr.)/alleviated (Alle.) water scarcity, and (right-hand side of dashed line) experiencing both increases and decreases in both frequency and average duration of water scarcity between two consecutive periods.

However, the dominant drivers of changes in WSI varied (Fig. 5). For example, the increased WSI in the western parts of Gansu, Ningxia and Henan provinces can mainly be ascribed to the rapid rise in irrigation from P1 to P2 (Fig. 5a). Additionally, water use by other sectors (industry, urban, and rural) was also the main reason for the increase in water stress in the central parts of the Loess Plateau. In contrast, water availability was the primary driver of changes in WSI in 178 sub-basins from P2 to P3 (Fig. 5b), underscoring the climatic controls on changes in water stress in these regions over the recent decades. Specifically, climate change contributed to a reduction in water stress in regions above Ningxia but exacerbated it in other parts of the YRB. Water withdrawals were responsible for the increased WSI in only 34 sub-basins.

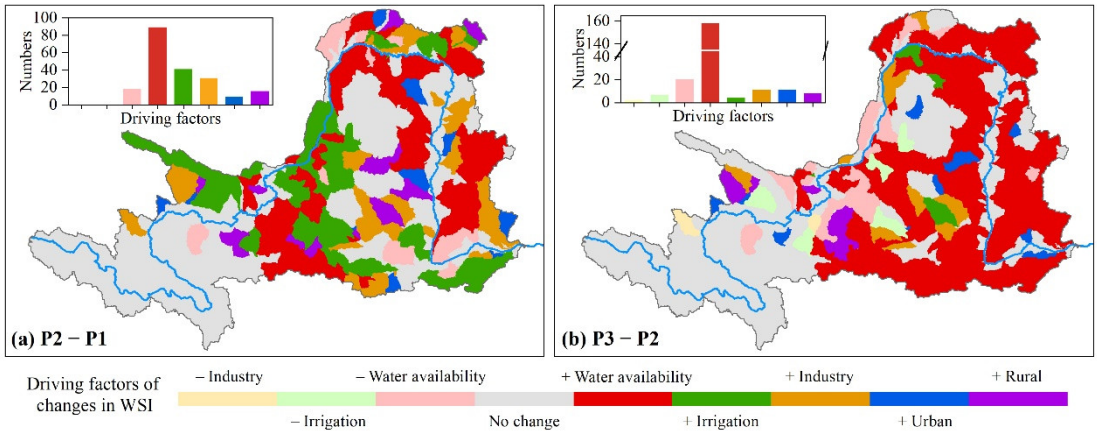

Figure 5. Driving factors of changes in WSI between two consecutive periods at the sub-basin scale. For the drivers, a '+' prefix indicates a positive effect on ΔWSI, whereas a '–' indicates a negative effect.

3.2. Important roles of local water availability and upstream flows

We further investigated the drivers of changes in total water availability in terms of local water availability, upstream flows, and upstream water consumption (see Equations 9–12). We found that upstream flows were responsible for changes in total water availability in 36%–43% (154–184) of the sub-basins (Fig. 6a), most of which were located along the main stem of the Yellow River (Fig. S6). The upper regions above Tangnaihai and Lanzhou hydrological stations had the largest shares of total natural flows of the study area (Huayuankou station), with mean annual ratios of 0.39 and 0.64, respectively. More importantly, these ratios consistently increased over the study period (Fig. 6b), suggesting that these regions have increasingly dominated the determination of total water resources of the whole YRB owing to climate change. However, this is also mostly beyond the control of local decision-makers.

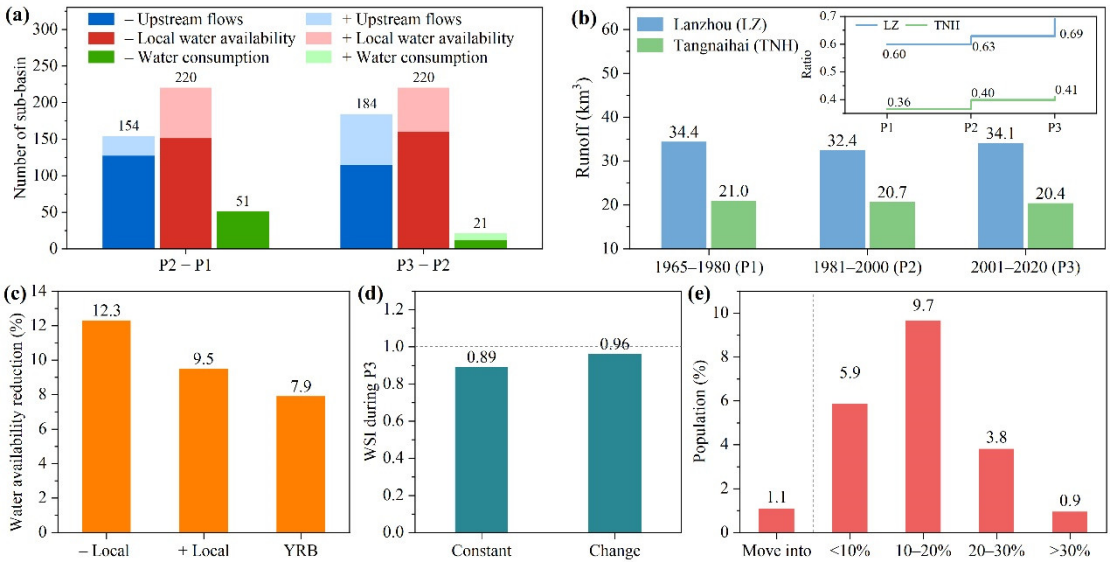

Figure 6. (a) Number of sub-basins experiencing different drivers of total water availability between two consecutive periods. For the drivers, a '+' prefix indicates a positive effect on water availability, whereas a '–' indicates a negative effect. (b) Runoff at the Tangnaihai (TNH) and Lanzhou (LZ) stations during different periods. The inset shows the runoff ratio of TNH and LZ to the Huayuankou station. (c) Reduction in water availability for sub-basins dominated by local water availability (− local and + local) and for the YRB with and without vegetation restoration. (d) WSI in P3 with (Change) and without (Constant) vegetation restoration. (e) Population moving into

435 water scarcity and experiencing aggravated water scarcity (increased WSI expressed as a percentage) owing to vegetation restoration.

The effects of local water resource management were also prominent in half of the sub-basins (220). Owing to the implementation of large-scale ecological restoration
440 projects (e.g., the Grain for Green Program) since the end of the 1990s, the vegetation coverage of the YRB has significantly improved and large amounts of cropland and barren land have been converted into forest and grassland (Figs. S7a–7c). However, the underlying surface changes reduced local water yield as a result of increased evapotranspiration (Fig. S7d). In terms of local water availability-dominant sub-basins,
445 land cover transitions led to a mean annual reduction in natural flows of 12.3%/9.5% (Fig. 6c). Over the entire basin, this generally decreased natural flows by 7.9% during P4, giving a corresponding regional WSI of 0.89 (Fig. 6d). Vegetation restorations led to 1.1% of the regional population moving into water scarcity and 10–20% increase in WSI for 9.7% of the total population (Fig. 6e). This implies that local vegetation
450 restoration in some places should be approached with caution to avoid water stress. For some sub-basins (less than 12%) where water availability is controlled by changes in upstream water consumption, integrated water management strategies, such as water resource recycling, should be considered to indirectly reduce water consumption and meet the water usage needs of downstream areas (Zhou et al., 2021).

455

3.3. Future water stress and potential solutions

As shown in Fig. 7a, regional total irrigation is projected to decrease by 13.3% in the 2030s compared to the recent two decades (P3). This decrease is mainly attributed to reductions in irrigation in northwestern parts of the YRB and central parts of the Loess
460 Plateau (Fig. 7b). With the development of industry and the rapid growth of urban population under different SSPs (Fig. S8), a general increase in industrial and urban water usage is projected. This increase is expected to be above 20% in most sub-basins

(despite a reduction in some areas) and over 100%, respectively (Figs. 7c, 7d, and S9). Rural water use has a moderate growth rate of 38% across five SSPs. In general, the total water use of the study area in the 2030s is projected to be 34.2 km^3 (6.5% higher than the current 32.1 km^3 during P3), 56.2% (19.2 km^3) of which will be contributed by irrigation (Fig. 7f). The industrial and urban sectors will account for the second-largest shares of total water use, with nearly equal proportions of 18.3% and 18.8%, respectively. The rural sector will have the smallest share (6.7%).

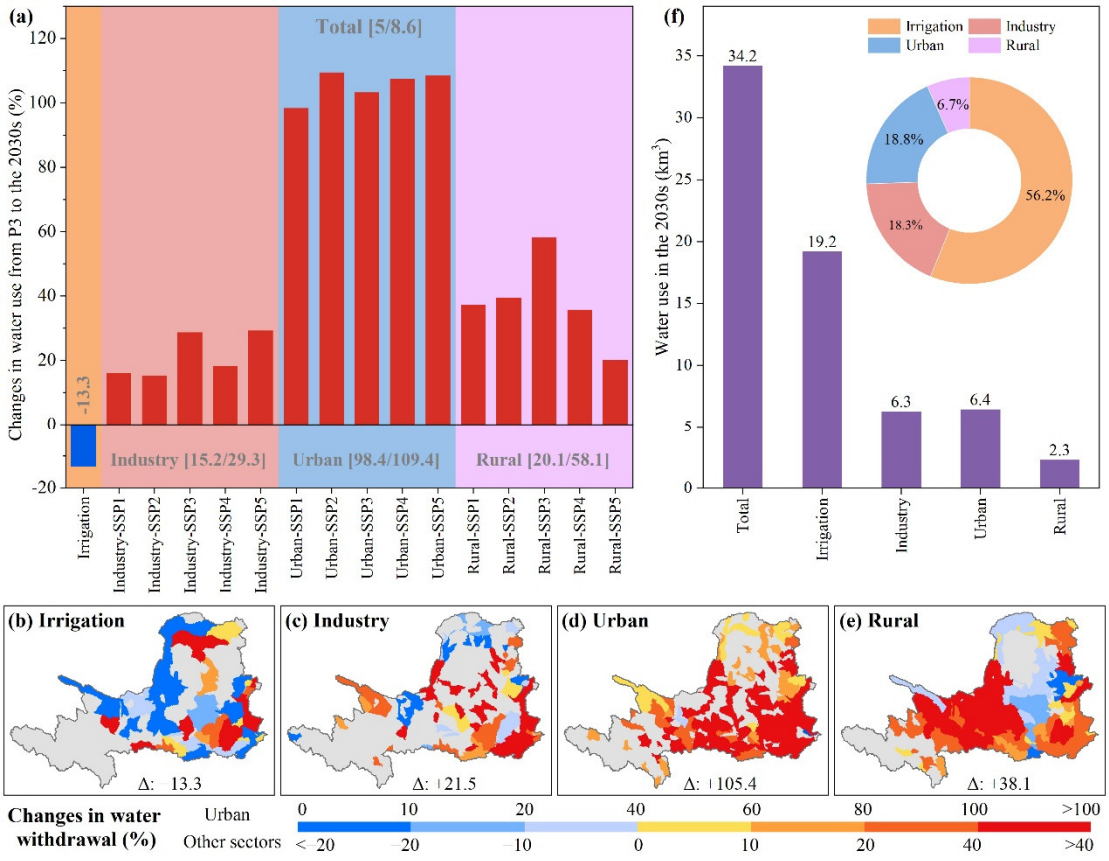

Figure 7. (a) Relative changes in water use of different sectors from the recent two decades (2001–2020) to the 2030s (%). The numbers in brackets are the minimum and maximum values for different SSPs. Panels (b-e) illustrate the spatial patterns of relative changes in sectoral water withdrawal. For the industrial, urban, and rural sectors, the mean annual values across five SSPs were used (see changes in individual SSP in Fig. S9). The numbers at the bottom indicate the values at the regional scale. (f) Water use in the 2030s and the proportion of use by different sectors (pie chart).

Further analysis showed that the surface water deficit of the YRB in the 2030s would be 0.6–8.36 km^3 in the absence of additional measures when considering sectoral water use with different priorities (Fig. 8a). When all sectoral water usages need to be fulfilled (8.36 km^3), the possible improvement of irrigation efficiency in the future could solve 25% of the water deficit (2.06 km^3), leading to a net surface water deficit of 6.3 km^3. From the perspective of water supply, the inter-basin water diversion project is regarded as an important measure to alleviate the severe water stress problems experienced in northern China. The Hanjiang-to-Weihe River (HWR) project and the South-to-North Water Diversion (SNWD) project are the two most important projects for the YRB. The total water coming from the HWR project to Guanzhong Plain and from the Middle Route of the SNWD project to Henan province (SN-HN) would be 5.27 km^3 (Fig. 8b). The planning Western Route of the SNWD project (SN-WR), which links the headwaters of the Yangtze and YRB, is 8 km^3 in the first phase. The implementation of irrigation water-saving strategies can effectively alleviate the water supply pressure of these external water diversion projects. In the 2030s, the WSI is projected to reach 1.02, i.e., water resources cannot sustain environmental or anthropogenic needs (Fig. 8c). However, improving irrigation efficiency could counterbalance the growth in water demand from other sectors and even reduce water stress below P3 level (0.95). As a result, water stress would decrease in the northwestern and northern regions, but it will increase further in most other areas, with some sub-basins experiencing WSI increases of more than 30% (Fig. 8d). Between the recent two decades and the 2030s, 42% (10.2%) and 2.9% (0.5%) of the population will experience aggravated (alleviated) and be moved into (out of) water scarcity conditions, respectively (Fig. 8e). An additional 4.5% of the total population would benefit from improvements in irrigation efficiency.

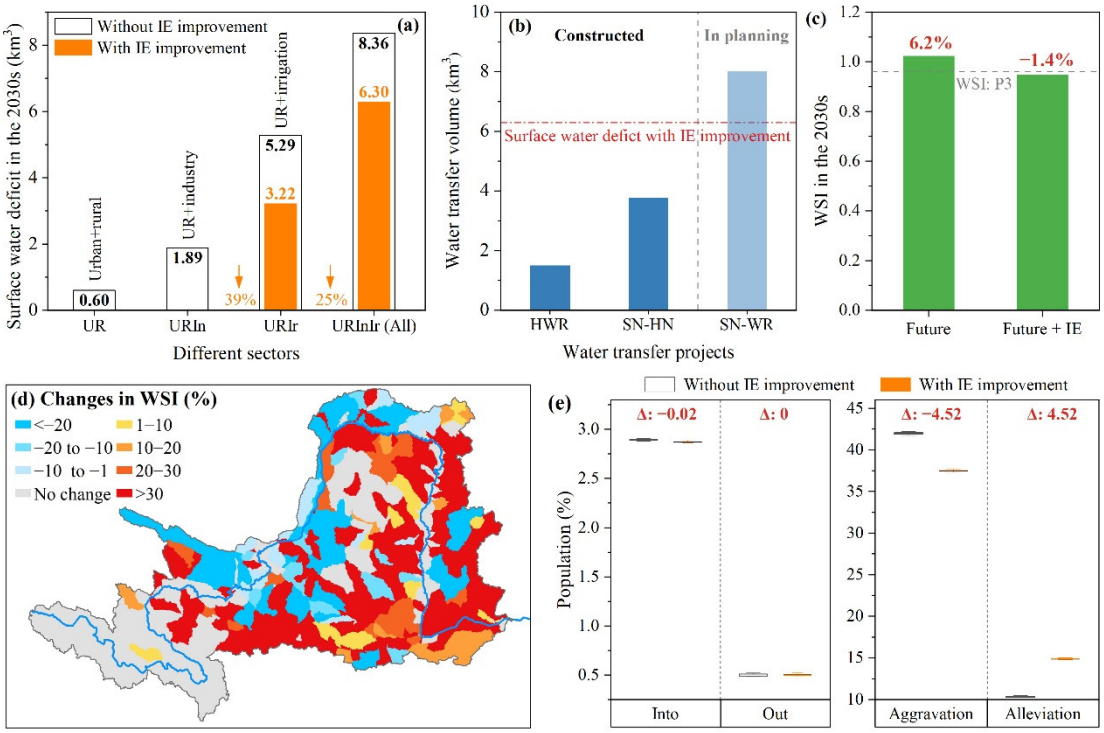

Figure 8. Impacts of improvement in irrigation efficiency (IE) on water stress alleviation in the 2030s. (a) Surface water deficit in the 2030s under different sectoral water demand. (b) Water transfer volumes to the study area from the HWR project, SNWD project to Henan Province (SN-HN), and Western Route of the SNWD project (SN-WR) in the first phase. (c) Future WSI with and without IE improvement. The red numbers are the relative change in WSI from P3 to the 2030s. (d) Spatial pattern of relative changes in WSI with IE improvement (from P3 to the 2030s). (e) Percentage of the population experiencing aggravated/alleviated water scarcity and moving into/out of water scarcity (from P3 to the 2030s).

4 Discussion

4.1. Water stress in the past and futures: comparison with other studies

Water stress hotspots were mainly concentrated in areas between the Lanzhou and Toudaoguai hydrological stations and in large cities with higher water demands (Fig. S4); this was similar to the findings of previous studies (Ma et al., 2020a; Xie et al., 2020; Sun et al., 2021). However, the severity of water stress was not the same as that

reported in previous studies because of the choice of different water withdrawals, water availability datasets, proportion of EFR, and even study period in the WSI estimation. We also found that water stress over the whole study area has generally intensified during the past few decades, which also generally corroborates previous findings at different scales (Liu et al., 2019; Zhou et al., 2019; Huang et al., 2021; Huang et al., 2023). Regarding the driving factors of changes in WSI, previous studies have concluded that rapid growth in water use was the primary factor leading to increased WSI in northern China over the past four decades (Wada et al., 2011; Huang et al., 2021). In contrast, increased water availability owing to enhanced precipitation was the main contributor to alleviating water stress in the YRB during 2001–2020 (Huang et al., 2023). These results were confirmed by our study (Fig. 4a). By using survey-based water withdrawal datasets and SWAT simulations, our study further isolated the contribution of water withdrawals by various water use sectors on the evolution of water stress at the sub-basin scale (Fig. 5), which was rarely considered in previous studies. We found that water withdrawals, particularly for irrigation and industrial water use, dominated the increase in WSI in the northwestern regions and the Loess Plateau before 2000. However, since 2000, China's State Council and Ministries have implemented a series of laws, regulations, action plans, and technology related to water conservation (Zhao et al., 2015; Zhou et al., 2020), especially the strict Three Red Lines in 2012. This led to a widespread stagnation and even a reduction in human water withdrawals in northern China (Huang et al., 2023), indicating the remarkable success of government-led water conservation efforts. As a result, human water use is no longer the main reason for the increased WSI in most sub-basins (Fig. 5b). Thus, a regional deceleration in the rate of WSI increase was observed (41.8% versus 21.4%) and the changes in WSI were driven almost equally by water withdrawals and water availability from P2 to P3 (Fig. 4a), underscoring the important role of climate change in influencing water stress under increasingly stringent water management strategies. Additionally, we found that the frequency and duration of water scarcity in the YRB and some sub-basins exceeded 0.5 and 6 months, respectively (Figs. 4b and S5), indicating that water scarcity occurred more than half the time at the monthly scale,

despite WSI being less than 1 at the decadal scale. These seasonal analyses can provide valuable scientific guidance for the planning of reservoirs and water diversion projects.

Because the decrease in irrigation water use was offset by an increase in water use from the other three sectors (industry, urban, and rural), the final total water use in the 2030s was predicted as 34.2 km^3 based on the trajectory of historical withdrawal and different SSPs (Fig. 7). When further water withdrawals of ~12 km^3 below the Huayuankou station (the lower reaches of the Yellow River) were taken into account (http://yrcc.gov.cn/gzfw/szygb/index.html), the total water demand of the entire YRB was approximately 46 km^3. This value is 10–20 km^3 lower than that reported by Yin et al. (2020), based on different global hydrological models (GHM) and SSP combinations. On the one hand, our analysis based on historical survey data showed that irrigation water use has presented a steady downward trend over the past 20 years, which was not often captured by large-scale GHMs (Haddeland et al., 2014; Liu et al., 2019). On the other hand, we calibrated the SSP predictions using the latest socio-economic data. Overall, we believe that including data from the most recent decade can incorporate the effect of water efficiency improvements and current water-saving technologies, thereby making water withdrawal predictions more reliable and providing valuable insights for policymakers. When water availability remained stable (constant at the 2001–2020 level), the water stress was projected to be further aggravated, which was also reported in earlier studies (Yin et al., 2017; Liu et al., 2019; Yang et al., 2023). For example, Omer et al. (2020) indicated that critical water scarcity would occur in the YRB if the current trend of water use continues in the near future. However, we found that if improvements in irrigation efficiency are taken into account, regional water stress could be maintained at its current level (0.95), a finding rarely reported previously.

4.2. Broader implications for water resources management

In terms of water supply, the upper YRB including the source regions (above the Tangnaihai station) provides a vital water source for the whole YRB. However, water

availability in this region is highly sensitive to global warming (Zhang et al., 2014; Kuang and Jiao, 2016; Ji et al., 2023), which can then further exert a considerable impact on the security of food, energy, and water in downstream regions (Cui et al., 2023). Meltwater from snow and glaciers can help mitigate water stress for both local and downstream areas. However, meltwater acting as an additional source of water is not sustainable in the long term (Wang et al., 2023). Influenced by global warming, the terrestrial water storage deficit is predicted to expand northwards on the Tibetan Plateau by the end of the century, which threatens the sustainability of water supplies in the upper YRB (Zhang et al., 2023b). Worse still, the acceleration of glacier mass loss may bring about a series of unintended and detrimental environmental and ecological consequences (Hugonnet et al., 2021). Therefore, it is necessary to urgently reduce carbon emissions and slow climate warming to alleviate the water stress of millions of people living downstream in the YRB.

Meanwhile, we found that total water availability in more than half of the sub-basins was controlled by local water yields (Fig. 6a), underscoring the importance of local water management strategies. Previous studies have shown that the impact of vegetation restoration on water availability exhibits significant spatial heterogeneity. It decreases water resources in arid areas (measured as precipitation minus evapotranspiration) but increases water resources in humid regions (Feng et al., 2017; Zan et al., 2024). Owing to several ambitious programs to conserve and expand forests (Bryan et al., 2018), vegetation greening of the YRB has been strikingly prominent during recent years (Zhang et al., 2023a); however, a strain on water resources has been observed in our study (Fig. S7) and many other previous studies (Feng et al., 2016; Wang et al., 2019; Zhang et al., 2023c; Yao et al., 2024). By scenario simulation, we estimated that vegetation restoration led to a reduction in runoff of 7.9% over the YRB during 2001–2020, thereby exacerbating water stress. This result is expected, given that most of the YRB is classified as arid or semi-arid. Similar findings have been reported from semi-arid and arid regions in China (Zhang et al., 2018), where vegetation restoration resulted in 8.5% and 11.7% reductions in runoff in the 1990s and 2000s,

respectively. In areas already experiencing a decrease in water availability induced by climate change, vegetation greening has undoubtedly exacerbated the water crisis. Therefore, to alleviate regional water stress, in addition to climate change adaptation strategies and substantial investment in hard-path infrastructure (e.g., water diversion project), nature-based solutions should also be considered. For example, controlling the scale of reforestation and conducting appropriate grazing activities in excessively restored grasslands (Liang et al., 2019; Deng et al., 2023) could potentially achieve a triple-win in economic development, ecological protection, and water resource security.

With changes in the economic structure and rapid urbanization, urban domestic water use is projected to equal or even exceed industrial water use by the 2030s, highlighting the importance of effective urban water resource management in alleviating future water stress. Irrigation still accounts for the largest share of total water use in the future; therefore, enhancing its efficiency will likely provide the most feasible solution for mitigating water stress in the YRB. The YRB is a water-scarce region where resolving the water shortage issue by focusing only on either the supply or demand perspective is challenging. We found that it will be almost impossible to meet both productive and domestic water demands through irrigation efficiency improvements alone in most sub-basins in the 2030s (Figures not shown). While relying on external inter-basin water transfer projects can significantly and directly mitigate water stress in the region, such measures should be approached with caution, as these large-scale infrastructures often have considerable ecological and social impacts (Webber et al., 2021; Liu et al., 2023). Improvements in irrigation efficiency can free up water resources and reduce 25% of the surface water deficit to meet all sectoral water demands, greatly alleviating the pressure on water diversion projects (Figs. 8a and 8b). Such efficiency gains would allow the water stress in the study area to be maintained at its current level (0.95) in the future (Fig. 8c), which is approaching the threshold of water scarcity (WSI =1). Given the great water demand in the lower reaches of the YRB (below the HYK station) and the task of supplying water to other basins (such as the Hai River), water scarcity is inevitable across the entire YRB. However, there is a positive development: since the

ecological protection and high-quality development of the Yellow River Basin was designated a national strategy in 2019, the Chinese government has implemented several proactive strategies in this basin. For instance, the implementation of the Yellow River Protection Law (2023) has legally constrained the intensity and total volume of water usage (http://en.npc.gov.cn.cdurl.cn/2022-10/30/c_954870.htm). Moreover, the recently planned Bailong River Water Diversion project is expected to provide 774 million cubic meters of water resources to Gansu and Shaanxi provinces in 2040 (https://www.mee.gov.cn/xxgk2018/xxgk/xxgk11/202307/t20230725_1037157.html). In summary, it will be necessary to implement a variety of adaptation measures on both the supply and demand sides to resolve the water crisis in the YRB.

4.3. Uncertainty

Our study contains several uncertainties. First, the impact of reservoirs was not considered in our study due to data inaccessibility at a finer time scale. Although of little impact on the decadal scale, this may result in overestimations of the frequency and duration of water scarcity. This is because there are many reservoirs in the YRB and occasionally monthly water scarcity in some sub-basins may be addressed or alleviated through seasonal flow regulations (Ma et al., 2020a; Ji et al., 2023). Second, in calculating water availability, we adopted the method widely used by previous estimates (Liu et al., 2019; Munia et al., 2020; He et al., 2021), which only considers the water resources in the river (see section 2.2). The water storage in lakes, aquifers, and groundwater, for which the absolute volumes were not known, was assumed to be in a state of equilibrium (Veldkamp et al., 2017; Huang et al., 2021). Thus, without considering groundwater pumping from deep aquifers, water availability may be underestimated in regions heavily dependent on such resources, potentially leading to a lower anticipated water stress level in reality. Moreover, the future WSI only considered the effects of water withdrawals and overlooked the impacts of climate change. Previous studies projected that changes in annual runoff in the YRB would not be evident in the near future during the period from 2000 to the 2030s (Yin et al. 2017;

Yin et al. 2020), but the long-term and seasonal climatic impacts should be considered in our further research.

Reclaimed water is regarded as an important alternative water source for cities (Liu et al., 2020; Hastie et al., 2022). As domestic water use continues to increase rapidly, the potential for reclaimed water utilization in the future is likely to be enormous. Previous analyses from China have shown that water reuse could alleviate up to 12% of the national water stress by 2030 (Chen et al., 2023). Thus, further studies are required to better incorporate these water resources in the YRB. Additionally, current water-saving technologies have already been widely adopted (Zhou et al., 2020). We considered the effects of improved irrigation efficiency in future water stress assessments, assuming that water management policies would be implemented effectively. However, as water use efficiency increases, the marginal cost of maintaining a decreasing trend in water use intensity increases (Sun, 2023). In other words, the sustained alleviation of water stress through improved water efficiency would entail higher economic costs in the future. The estimation of water availability and thus the WSI largely depends on the chosen method for determining EFR (Liu et al., 2021). A higher EFR ratio results in higher water stress, and vice versa. However, identifying an appropriate EFR method to assess water stress is beyond the scope of this study.

5 Conclusions

This study presents an integrated analytical framework to reveal a comprehensive picture of a given water crisis in the YRB, including multiple water stress indicators, driving factors of changes in WSI, and future predictions of water stress along with potential feasible solutions. Generally speaking, analysis of critical indicators (WSI, frequency, duration, and exposed population of water scarcity) shows that the water supply and demand situation in the YRB has evolved in an unfavorable direction during 1965–2020. Compared with the period before 1980, the regional WSI, frequency, and

duration of water scarcity increased by 76%, 100%, and 92%, respectively, over the past two decades. Water withdrawal and water availability induced by climate change contributed to a 36.8% and 5% increase in WSI, respectively, from P1 to P2. In contrast, these contributions were 10.4% and 11%, respectively, from P2 to P3. At the sub-basin scale, irrigation was the primary factor driving WSI increases in the western parts of Gansu, Ningxia, and Henan provinces before 2000. Additionally, water use in other sectors (industry, urban, and rural) was the main reason for the rise in water stress in the central regions of the Loess Plateau. In contrast, water availability was responsible for the changes in WSI in most of the sub-basins during the most recent decades studied. Meanwhile, further analysis showed that upstream flows and local water yields were the main factors contributing to changes in total water availability at the sub-basin scale. Pressure from upstream regions of the YRB on downstream water use has gradually increased and will be unsustainable in the future. Vegetation restoration led to a reduction in natural flow of 7.9% after 2000, aggravating regional water shortages.

Based on the historical trajectory of irrigation water use and the corrected socio-economic data under different SSPs, we predict that the total water demand in the study area during the 2030s will be 6.5% higher than in P3 (34.2 km^3). This increase largely resulted from increased urban and industrial use, partly offset by reduced irrigation. Considering sectoral water use with different priorities, the surface water deficit in the study area is predicted to range from 0.6 to 8.36 km^3. The potential improvement in irrigation efficiency could resolve 25% of this maximum water deficit (all sector demands are met), leading to a net surface water deficit of 6.3 km^3. This reduction would greatly alleviate the water supply pressure on external inter-basin water transfer projects. Such efficiency gains would allow the water stress in the study area to be maintained at its current level (0.95) in the future. Under these conditions, the water crisis is expected to worsen for 44.9% of the total population and ease for 10.7%. Given the great water demand in the lower reaches of the Yellow River (below the HYK station) and the task of supplying water to other basins, it is essential to combine water supply- and demand-oriented measures to address the water crisis in the YRB. The

results of this study have important implications for coping with water scarcity not only in the YRB but also in other basins facing similar situations.

Data availability

Data will be made available on request (baoqzhang@lzu.edu.cn).

Author contributions

Weibin Zhang: Conceptualization, Data curation, Formal analysis, Methodology, Validation, Visualization, Writing - original draft. *Xining Zhao*: Conceptualization, Funding acquisition, Validation, Resources, Writing - Review. *Xuerui Gao*: Data curation, Methodology, Writing - Review. *Wei Liang*: Conceptualization, Methodology, Validation. *Junyi Li*: Formal analysis, Resources, Writing - Review. *Baoqing Zhang*: Conceptualization, Formal analysis, Funding acquisition, Writing - Review and Editing.

Competing interests

The authors declare that they have no known competing financial interests or personal relationships that could have appeared to influence the work reported in this paper.

Acknowledgments

This research was jointly supported by National Natural Science Foundation of China (NSFC) (42125705 and 42041004), National Key Research and Development Program of China (2021YFD1900700), and Fundamental Research Funds for the Central Universities (lzujbky-2023-eyt01 and lzujbky-2023-ey09). Wei Liang would like to acknowledge support from the NSFC (42071144). We also thank the editors and anonymous reviewers for constructive comments, which helped us to improve the manuscript substantially. Partial data are provided by the Cold and Arid Regions Critical Zone Hydrological Cycle Observation Network, Management Center of Scientific Observing Stations, Lanzhou University. This work is also supported by the Supercomputing Center of Lanzhou University.

References

Albers, L. T., Schyns, J. F., Booij, M. J., and Zhuo, L.: Blue water footprint caps per sub-catchment to mitigate water scarcity in a large river basin: The case of the Yellow River in China, J. Hydrol., 603, 126992, https://doi.org/10.1016/j.jhydrol.2021.126992, 2021.

Bryan, B. A., Gao, L., Ye, Y., Sun, X., Connor, J. D., Crossman, N. D., Stafford-Smith, M., Wu, J., He, C., Yu, D., Liu, Z., Li, A., Huang, Q., Ren, H., Deng, X., Zheng, H., Niu, J., Han, G., and Hou, X.: China's response to a national land-system sustainability emergency, Nature, 559, 193-204, 10.1038/s41586-018-0280-2, 2018.

Chen, S., Zhang, L., Liu, B., Yi, H., Su, H., Kharrazi, A., Jiang, F., Lu, Z., Crittenden, J. C., and Chen, B.: Decoupling wastewater-related greenhouse gas emissions and water stress alleviation across 300 cities in China is challenging yet plausible by 2030, Nature Water, 1, 534-546, 10.1038/s44221-023-00087-4, 2023.

Cui, T., Li, Y., Yang, L., Nan, Y., Li, K., Tudaji, M., Hu, H., Long, D., Shahid, M., Mubeen, A., He, Z., Yong, B., Lu, H., Li, C., Ni, G., Hu, C., and Tian, F.: Non-monotonic changes in Asian Water Towers' streamflow at increasing warming levels, Nat. Commun., 14, 1176, 10.1038/s41467-023-36804-6, 2023.

Degefu, D. M., Weijun, H., Zaiyi, L., Liang, Y., Zhengwei, H., and Min, A.: Mapping monthly water scarcity in global transboundary basins at country-basin mesh based spatial resolution, Sci. Rep., 8, 2144, 10.1038/s41598-018-20032-w, 2018.

Deng, L., Shangguan, Z., Bell, S. M., Soromotin, A. V., Peng, C., An, S., Wu, X., Xu, X., Wang, K., Li, J., Tang, Z., Yan, W., Zhang, F., Li, J., Wu, J., and Kuzyakov, Y.: Carbon in Chinese grasslands: meta-analysis and theory of grazing effects, Carbon Research, 2, 19, 10.1007/s44246-023-00051-7, 2023.

Feng, H., Zou, B., and Luo, J.: Coverage-dependent amplifiers of vegetation change on global water cycle dynamics, J. Hydrol., 550, 220-229, https://doi.org/10.1016/j.jhydrol.2017.04.056, 2017.

Feng, X., Fu, B., Piao, S., Wang, S., Ciais, P., Zeng, Z., Lu, Y., Zeng, Y., Li, Y., Jiang,

X., and Wu, B.: Revegetation in China's Loess Plateau is approaching sustainable water resource limits, Nat. Clim. Change, 6, 1019-1022, 10.1038/nclimate3092, 2016.

Florke, M., Kynast, E., Barlund, I., Eisner, S., Wimmer, F., and Alcamo, J.: Domestic and industrial water uses of the past 60 years as a mirror of socio-economic development: A global simulation study, Global Environ. Change, 23, 144-156, 2013.

Greve, P., Kahil, T., Mochizuki, J., Schinko, T., Satoh, Y., Burek, P., Fischer, G., Tramberend, S., Burtscher, R., Langan, S., and Wada, Y.: Global assessment of water challenges under uncertainty in water scarcity projections, Nat. Sustain., 1, 486-494, 10.1038/s41893-018-0134-9, 2018.

Haddeland, I., Heinke, J., Biemans, H., Eisner, S., Flörke, M., Hanasaki, N., Konzmann, M., Ludwig, F., Masaki, Y., Schewe, J., Stacke, T., Tessler, Z. D., Wada, Y., and Wisser, D.: Global water resources affected by human interventions and climate change, Proc. Natl. Acad. Sci. USA, 111, 3251-3256, 10.1073/pnas.1222475110, 2014.

Han, S., Leng, G., and Yu, L.: Review of Quantitative Applications of the Concept of the Water Planetary Boundary at Different Spatial Scales, Water Resour. Res., 59, e2022WR033646, https://doi.org/10.1029/2022WR033646, 2023.

Hanasaki, N., Fujimori, S., Yamamoto, T., Yoshikawa, S., Masaki, Y., Hijioka, Y., Kainuma, M., Kanamori, Y., Masui, T., Takahashi, K., and Kanae, S.: A global water scarcity assessment under Shared Socio-economic Pathways – Part 1: Water use, Hydrol. Earth Syst. Sci., 17, 2375-2391, 10.5194/hess-17-2375-2013, 2013.

Hastie, A. G., Otrubina, V. V., and Stillwell, A. S.: Lack of Clarity Around Policies, Data Management, and Infrastructure May Hinder the Efficient Use of Reclaimed Water Resources in the United States, ACS ES&T Water, 2, 2289-2296, 10.1021/acsestwater.2c00307, 2022.

He, C., Liu, Z., Wu, J., Pan, X., Fang, Z., Li, J., and Bryan, B. A.: Future global urban water scarcity and potential solutions, Nat. Commun., 12, 4667, 10.1038/s41467-

021-25026-3, 2021.

Huang, Z., Hejazi, M., Li, X., Tang, Q., Vernon, C., Leng, G., Liu, Y., Döll, P., Eisner, S., Gerten, D., Hanasaki, N., and Wada, Y.: Reconstruction of global gridded monthly sectoral water withdrawals for 1971–2010 and analysis of their spatiotemporal patterns, Hydrol. Earth Syst. Sci., 22, 2117-2133, 10.5194/hess-22-2117-2018, 2018.

Huang, Z., Yuan, X., and Liu, X.: The key drivers for the changes in global water scarcity: Water withdrawal versus water availability, J. Hydrol., 601, 126658, https://doi.org/10.1016/j.jhydrol.2021.126658, 2021.

Huang, Z., Yuan, X., Liu, X., and Tang, Q.: Growing control of climate change on water scarcity alleviation over northern part of China, Journal of Hydrology: Regional Studies, 46, 101332, https://doi.org/10.1016/j.ejrh.2023.101332, 2023.

Hugonnet, R., McNabb, R., Berthier, E., Menounos, B., Nuth, C., Girod, L., Farinotti, D., Huss, M., Dussaillant, I., Brun, F., and Kääb, A.: Accelerated global glacier mass loss in the early twenty-first century, Nature, 592, 726-731, 10.1038/s41586-021-03436-z, 2021.

Ji, P., Yuan, X., and Jiao, Y.: Future hydrological drought changes over the upper Yellow River basin: The role of climate change, land cover change and reservoir operation, J. Hydrol., 617, 129128, https://doi.org/10.1016/j.jhydrol.2023.129128, 2023.

Kuang, X., and Jiao, J. J.: Review on climate change on the Tibetan Plateau during the last half century, J. Geophys. Res.: Atmos., 121, 3979-4007, https://doi.org/10.1002/2015JD024728, 2016.

Liang, W., Fu, B., Wang, S., Zhang, W., Jin, Z., Feng, X., Yan, J., Liu, Y., and Zhou, S.: Quantification of the ecosystem carrying capacity on China's Loess Plateau, Ecol. Indicators, 101, 192-202, https://doi.org/10.1016/j.ecolind.2019.01.020, 2019.

Liu, L., Lopez, E., Dueñas-Osorio, L., Stadler, L., Xie, Y., Alvarez, P. J. J., and Li, Q.: The importance of system configuration for distributed direct potable water reuse, Nat. Sustain., 3, 548-555, 10.1038/s41893-020-0518-5, 2020.

Liu, X., Liu, W., Liu, L., Tang, Q., Liu, J., and Yang, H.: Environmental flow requirements largely reshape global surface water scarcity assessment,

Environmental Research Letters, 16, 104029, 10.1088/1748-9326/ac27cb, 2021.

Liu, X., Tang, Q., Liu, W., Veldkamp, T. I. E., Boulange, J., Liu, J., Wada, Y., Huang, Z., and Yang, H.: A spatially explicit assessment of growing water stress in China from the past to the future, Earth's Future, 7, 1027-1043, https://doi.org/10.1029/2019EF001181, 2019.

Liu, Y., Xin, Z., Sun, S., Zhang, C., and Fu, G.: Assessing environmental, economic, and social impacts of inter-basin water transfer in China, J. Hydrol., 625, 130008, 10.1016/j.jhydrol.2023.130008, 2023.

Long, D., Yang, W., Scanlon, B. R., Zhao, J., Liu, D., Burek, P., Pan, Y., You, L., and Wada, Y.: South-to-North Water Diversion stabilizing Beijing's groundwater levels, Nat. Commun., 11, 3665, 10.1038/s41467-020-17428-6, 2020.

Ma, T., Sun, S., Fu, G., Hall, J. W., Ni, Y., He, L., Yi, J., Zhao, N., Du, Y., Pei, T., Cheng, W., Song, C., Fang, C., and Zhou, C.: Pollution exacerbates China's water scarcity and its regional inequality, Nat. Commun., 11, 650, 10.1038/s41467-020-14532-5, 2020a.

Ma, Z. G., Fu, C. B., Zhou, T. J., Li, M. X., Zheng, Z. Y., Chen, L., Lv, M. X., and Yan, Z. W.: Status and ponder of climate and hydrology changes in the Yellow River Basin, Bulletin of Chinese Academy of Sciences, 35, 52-60, 10.16418/j.issn.1000-3045.20191223002, 2020b.

McDonald, R. I., Green, P., Balk, D., Fekete, B. M., Revenga, C., Todd, M., and Montgomery, M.: Urban growth, climate change, and freshwater availability, Proc. Natl. Acad. Sci. USA, 108, 6312-6317, doi:10.1073/pnas.1011615108, 2011.

Mekonnen, M. M., and Hoekstra, A. Y.: Four billion people facing severe water scarcity, Sci. Adv., 2, e1500323, doi:10.1126/sciadv.1500323, 2016.

Munia, H. A., Guillaume, J. H. A., Wada, Y., Veldkamp, T., Virkki, V., and Kummu, M.: Future transboundary water stress and its drivers under climate change: a global study, Earth's Future, 8, e2019EF001321, https://doi.org/10.1029/2019EF001321, 2020.

Niu, C., Chang, J., Wang, Y., Shi, X., Wang, X., Guo, A., Jin, W., and Zhou, S.: A Water Resource Equilibrium Regulation Model Under Water Resource Utilization

Conflict: A Case Study in the Yellow River Basin, Water Resour. Res., 58, e2021WR030779, https://doi.org/10.1029/2021WR030779, 2022.

Oki, T., and Kanae, S.: Global hydrological cycles and world water resources, Science, 313, 1068-1072, doi:10.1126/science.1128845, 2006.

Omer, A., Elagib, N. A., Zhuguo, M., Saleem, F., and Mohammed, A.: Water scarcity in the Yellow River Basin under future climate change and human activities, Sci. Total Environ., 749, 141446, https://doi.org/10.1016/j.scitotenv.2020.141446, 2020.

Pastor, A. V., Ludwig, F., Biemans, H., Hoff, H., and Kabat, P.: Accounting for environmental flow requirements in global water assessments, Hydrol. Earth Syst. Sci., 18, 5041-5059, 10.5194/hess-18-5041-2014, 2014.

Porkka, M., Gerten, D., Schaphoff, S., Siebert, S., and Kummu, M.: Causes and trends of water scarcity in food production, Environmental Research Letters, 11, 015001, 10.1088/1748-9326/11/1/015001, 2016.

Qin, Y.: Global competing water uses for food and energy, Environmental Research Letters, 16, 064091, 10.1088/1748-9326/ac06fa, 2021.

Qin, Y., Mueller, N. D., Siebert, S., Jackson, R. B., AghaKouchak, A., Zimmerman, J. B., Tong, D., Hong, C., and Davis, S. J.: Flexibility and intensity of global water use, Nat. Sustain., 2, 515-523, 10.1038/s41893-019-0294-2, 2019.

Rodell, M., and Li, B.: Changing intensity of hydroclimatic extreme events revealed by GRACE and GRACE-FO, Nature Water, 1, 241-248, 10.1038/s44221-023-00040-5, 2023.

Scanlon, B. R., Fakhreddine, S., Rateb, A., de Graaf, I., Famiglietti, J., Gleeson, T., Grafton, R. Q., Jobbagy, E., Kebede, S., Kolusu, S. R., Konikow, L. F., Long, D., Mekonnen, M., Schmied, H. M., Mukherjee, A., MacDonald, A., Reedy, R. C., Shamsudduha, M., Simmons, C. T., Sun, A., Taylor, R. G., Villholth, K. G., Vörösmarty, C. J., and Zheng, C.: Global water resources and the role of groundwater in a resilient water future, Nature Reviews Earth & Environment, 4, 87-101, 10.1038/s43017-022-00378-6, 2023.

Schewe, J., Heinke, J., Gerten, D., Haddeland, I., Arnell, N. W., Clark, D. B., Dankers,

R., Eisner, S., Fekete, B. M., and Colóngonzález, F. J.: Multimodel assessment of water scarcity under climate change, Proc. Natl. Acad. Sci. USA, 111, 3245, 2014.

Song, S., Wang, S., Wu, X., Wei, Y., Cumming, G. S., Qin, Y., Wu, X., and Fu, B.: Identifying regime transitions for water governance in the Yellow River Basin, China, Water Resour. Res., 59, e2022WR033819, https://doi.org/10.1029/2022WR033819, 2023.

Sun, S.: Water use efficiency evolution in the Yellow River Basin: an integrated analysis of spatial-temporal decomposition, Hydrol. Sci. J., 68, 119-130, 10.1080/02626667.2022.2150552, 2023.

Sun, S., Zhou, X., Liu, H., Jiang, Y., Zhou, H., Zhang, C., and Fu, G.: Unraveling the effect of inter-basin water transfer on reducing water scarcity and its inequality in China, Water Res., 194, 116931, https://doi.org/10.1016/j.watres.2021.116931, 2021.

Tang, Y., Tang, Q., Tian, F., Zhang, Z., and Liu, G.: Responses of natural runoff to recent climatic variations in the Yellow River basin, China, Hydrol. Earth Syst. Sci., 17, 4471-4480, 10.5194/hess-17-4471-2013, 2013.

UNEP: Options for Decoupling Economic Growth from Water use and Water Pollution (https://www.resourcepanel.org/file/342/download?token=LmsRBoq4), 2015.

Veldkamp, T. I. E., Wada, Y., Aerts, J. C. J. H., Döll, P., Gosling, S. N., Liu, J., Masaki, Y., Oki, T., Ostberg, S., Pokhrel, Y., Satoh, Y., Kim, H., and Ward, P. J.: Water scarcity hotspots travel downstream due to human interventions in the 20th and 21st century, Nat. Commun., 8, 15697, 10.1038/ncomms15697, 2017.

Wada, Y., de Graaf, I. E. M., and van Beek, L. P. H.: High-resolution modeling of human and climate impacts on global water resources, Journal of Advances in Modeling Earth Systems, 8, 735-763, https://doi.org/10.1002/2015MS000618, 2016a.

Wada, Y., Florke, M., Hanasaki, N., Eisner, S., Fischer, G., Tramberend, S., Satoh, Y., Van Vliet, M., Yillia, P., and Ringler, C.: Modeling global water use for the 21st century: the Water Futures and Solutions (WFaS) initiative and its approaches, Geoscientific Model Development, 9, 175-222, 2016b.

Wada, Y., van Beek, L. P. H., and Bierkens, M. F. P.: Modelling global water stress of

the recent past: on the relative importance of trends in water demand and climate variability, Hydrol. Earth Syst. Sci., 15, 3785-3808, 10.5194/hess-15-3785-2011, 2011.

Wang, F., Duan, K., Fu, S., Gou, F., Liang, W., Yan, J., and Zhang, W.: Partitioning climate and human contributions to changes in mean annual streamflow based on the Budyko complementary relationship in the Loess Plateau, China, Sci. Total Environ., 665, 579-590, https://doi.org/10.1016/j.scitotenv.2019.01.386, 2019.

Wang, J., Li, Y., Huang, J., Yan, T., and Sun, T.: Growing water scarcity, food security and government responses in China, Global Food Security, 14, 9-17, https://doi.org/10.1016/j.gfs.2017.01.003, 2017.

Wang, T., Yang, D., Yang, Y., Zheng, G., Jin, H., Yao, T., and Cheng, G.: Unsustainable water supply from thawing permafrost on the Tibetan Plateau in a changing climate, Science Bulletin, 68, 10.1016/j.scib.2023.04.037, 2023.

Wang, X., Xiao, X., Zou, Z., Dong, J., Qin, Y., Doughty, R. B., Menarguez, M. A., Chen, B., Wang, J., Ye, H., Ma, J., Zhong, Q., Zhao, B., and Li, B.: Gainers and losers of surface and terrestrial water resources in China during 1989–2016, Nat. Commun., 11, 3471, 10.1038/s41467-020-17103-w, 2020.

Webber, M., Han, X., Rogers, S., Wang, M., Jiang, H., Zhang, W., Barnett, J., and Zhen, N.: Inside-out: Chinese academic assessments of large-scale water infrastructure, WIREs Water, 8, e1556, https://doi.org/10.1002/wat2.1556, 2021.

Xie, P., Zhuo, L., Yang, X., Huang, H., Gao, X., and Wu, P.: Spatial-temporal variations in blue and green water resources, water footprints and water scarcities in a large river basin: A case for the Yellow River basin, J. Hydrol., 590, 125222, https://doi.org/10.1016/j.jhydrol.2020.125222, 2020.

Xu, Z., Cheng, L., Liu, P., Hou, Q., Cheng, S., Qin, S., Liu, L., and Xia, J.: Investigating the spatial variability of water security risk and its driving mechanisms in China using machine learning, Journal of Cleaner Production, 362, 132303, https://doi.org/10.1016/j.jclepro.2022.132303, 2022.

Yang, Y., Chen, S., Zhou, Y., Ma, G., Huang, W., and Zhu, Y.: Method for quantitatively assessing the impact of an inter-basin water transfer project on ecological

environment-power generation in a water supply region, J. Hydrol., 618, 129250, https://doi.org/10.1016/j.jhydrol.2023.129250, 2023.

Yao, C., Zhang, H., Zhang, S., Dang, C., Mu, D., Zhang, Y., and Lyu, F.: A categorical quantification of the effects of vegetation restorations on streamflow variations in the Loess Plateau, China, J. Hydrol., 628, 130577, https://doi.org/10.1016/j.jhydrol.2023.130577, 2024.

Yin, Y., Tang, Q., Liu, X., and Zhang, X.: Water scarcity under various socio-economic pathways and its potential effects on food production in the Yellow River basin, Hydrol. Earth Syst. Sci., 21, 1-29, 10.5194/hess-21-791-2017, 2017.

Yin, Y., Wang, L., Wang, Z., Tang, Q., Piao, S., Chen, D., Xia, J., Conradt, T., Liu, J., Wada, Y., Cai, X., Xie, Z., Duan, Q., Li, X., Zhou, J., and Zhang, J.: Quantifying water scarcity in Northern China within the context of climatic and societal changes and South-to-North Water Diversion, Earth's Future, 8, e2020EF001492, https://doi.org/10.1029/2020EF001492, 2020.

Zan, B., Ge, J., Mu, M., Sun, Q., Luo, X., and Wei, J.: Spatiotemporal inequality in land water availability amplified by global tree restoration, Nature Water, 2, 863-874, 10.1038/s44221-024-00296-5, 2024.

Zhang, B., Tian, L., He, C., and He, X.: Response of erosive precipitation to vegetation restoration and its effect on soil and water conservation over China's Loess Plateau, Water Resour. Res., 59, 10.1029/2022WR033382, 2023a.

Zhang, Q., Shen, Z., Pokhrel, Y., Farinotti, D., Singh, V. P., Xu, C.-Y., Wu, W., and Wang, G.: Oceanic climate changes threaten the sustainability of Asia’s water tower, Nature, 615, 87-93, 10.1038/s41586-022-05643-8, 2023b.

Zhang, S., Yang, Y., McVicar, T., and Yang, D.: An analytical solution for the impact of vegetation changes on hydrological partitioning within the Budyko framework, Water Resour. Res., 54, 10.1002/2017WR022028, 2018.

Zhang, W., Liang, W., Gao, X., Li, J., and Zhao, X.: Trajectory in water scarcity and potential water savings benefits in the Yellow River basin, J. Hydrol., 130998, https://doi.org/10.1016/j.jhydrol.2024.130998, 2024.

Zhang, W., Liang, W., Tian, L., and Zhao, X.: Climatic and different human influences

on annual and seasonal streamflow with considering the soil water storage change in the middle reaches of the Yellow River basin, China, J. Hydrol., 619, 129298, https://doi.org/10.1016/j.jhydrol.2023.129298, 2023c.

Zhang, W., Zha, X., Li, J., Liang, W., Ma, Y., Fan, D., and Li, S.: Spatiotemporal change of blue water and green water resources in the Headwater of Yellow River Basin, China, Water Resour. Manage., 28, 4715-4732, 10.1007/s11269-014-0769-x, 2014.

Zhao, X., Liu, J., Liu, Q., Tillotson, M. R., Guan, D., and Hubacek, K.: Physical and virtual water transfers for regional water stress alleviation in China, Proc. Natl. Acad. Sci. USA, 112, 1031-1035, doi:10.1073/pnas.1404130112, 2015.

Zhou, F., Bo, Y., Ciais, P., Dumas, P., Tang, Q., Wang, X., Liu, J., Zheng, C., Polcher, J., Yin, Z., Guimberteau, M., Peng, S., Ottle, C., Zhao, X., Zhao, J., Tan, Q., Chen, L., Shen, H., Yang, H., Piao, S., Wang, H., and Wada, Y.: Deceleration of China's human water use and its key drivers, Proc. Natl. Acad. Sci. USA, 117, 7702, 10.1073/pnas.1909902117, 2020.

Zhou, X., Polcher, J., and Dumas, P.: Representing human water management in a land surface model using a supply/demand approach, Water Resour. Res., 57, 10.1029/2020WR028133, 2021.

Zhou, X., Yang, Y., Sheng, Z., and Zhang, Y.: Reconstructed natural runoff helps to quantify the relationship between upstream water use and downstream water scarcity in China's river basins, Hydrol. Earth Syst. Sci., 23, 2491-2505, 10.5194/hess-23-2491-2019, 2019.

Zhuo, L., Mekonnen, M. M., Hoekstra, A. Y., and Wada, Y.: Inter- and intra-annual variation of water footprint of crops and blue water scarcity in the Yellow River basin (1961–2009), Advances in Water Resources, 87, 29-41, https://doi.org/10.1016/j.advwatres.2015.11.002, 2016.